MICRO-THERMAL FIELD-FLOW FRACTIONATION

Josef JANČA

Université de La Rochelle, Pôle Sciences et Technologie, Avenue Michel Crépeau, 17042 La Rochelle Cedex 01, France; e-mail: jjanca@univ-lr.fr

Received May 27, 2002
Accepted August 30, 2002

The effect of miniaturization of the separation channel on the performance of thermal field-flow fractionation (TFFF) is substantiated theoretically. The experiments carried out under carefully chosen experimental conditions proved the high performance of the separation of polymers within an extended range of molar masses from relatively low up to ultrahigh-molar-mass (UHMM) samples. The new micro-TFFF allows to achieve high resolution when applying constant field force operation, it makes easy the programming of the temperature drop which is an advantageous operational mode from the point of view of the time of analysis, and it extends considerably the range of perfectly controlled temperature of the cold wall due to a substantial decrease in the heat energy flux compared with standard size channels.

Keywords: Miniaturized thermal FFF; Temperature drop programming; Separation channels; Cold wall temperature effect; Polymers; Separation.

Thermal field-flow fractionation (TFFF) is the oldest of all FFF methods[1]. It has been used for numerous separations, analyses and characterizations of polymers and colloidal particles[2,3]. The only experimental study whose goal was to increase the performance of the TFFF by reducing the thickness of the channel was published by Giddings *et al.*[4] and the effect of the reduced dimensions of the FFF channel on the performance of separation was studied later by Giddings[5], nevertheless, recently utilized separation channels[6,7] have almost the same size and design as those constructed at the very beginning. The new versatile micro-TFFF channel was built up just recently[8] and its performance was demostrated by several fractionations of polymer samples. Another construction of a microfabricated TFFF system was only introduced[9] but without any theoretical reasoning or a practical demonstration of an advantage of such a miniaturization. The only one separation of two polystyrene latexes[9] was rather problematic.

The main intention of this study was to demonstrate experimentally the effect of the miniaturization of the TFFF channel on the performance of

separation. The most important advantage of our micro-TFFF, substantiated theoretically, is the crucial extension of the range of perfectly controlled cold wall temperatures and of the temperature drops that can be reached due to the reduced heat flux. The demonstration of this potential of our micro-TFFF will be given by the investigation of the effect of the cold wall temperature on the retention and resolution of polystyrene (PS) samples down to as low temperature as 275 K. The additional advantages of our micro-TFFF are the possibility of on-line coupling with the mass spectroscopy which can allow a more detailed analysis of the fractionated species and a dramatic decrease in the amount of the fractionated sample down to few nanograms. As a result, the manipulation of the operational parameters and experimental conditions is much easier with our versatile micro-TFFF channel.

THEORY

The efficiency in FFF is described by the height equivalent to a theoretical plate[10]

$$H = \frac{2D}{R\langle v\rangle} + \frac{\chi w^2 \langle v\rangle}{D} + \sum H_i \ , \qquad (1)$$

where D is the diffusion coefficient of the fractionated species, R is the retention ratio, $\langle v\rangle$ is the average velocity of the carrier liquid, w is the thickness of the channel, the sum of H_i represents the extra-channel contributions to the plate height, and χ is a dimensionless parameter which is a complex function[11] of the retention parameter $\lambda = l/w$, where l is the distance between the accumulation wall and the center of gravity of the concentration distribution of the retained species across the channel. The retention parameter λ is related to the retention ratio R by[10]

$$R = 6\lambda[\coth(1/2\,\lambda) - 2\lambda] = V_0/V_R \ , \qquad (2)$$

where V_0 is the elution volume of an unretained species which is equal to the void volume of the channel and V_R is the retention volume of a retained species. The Eq. (*2*) holds accurately for isoviscous flow which is not the case in TFFF channels[2], however, the deviation from such an ideal behaviour has no significance for the purpose of this work. An optimum average velocity of the carrier liquid corresponding to the minimum of the $H = f(\langle v\rangle)$ function is[8]

$$\langle v \rangle_{\mathrm{opt}} = \frac{D}{w}\sqrt{\frac{2}{\chi R}} \,. \qquad (3)$$

The $\langle v \rangle_{\mathrm{opt}}$ reaches the values of the order of 0.01 cm/s for the macromolecules retained under the most currently used experimental conditions and decreases with increasing λ and w. A decrease in the channel thickness w leads to a decrease in H according to Eq. (*1*) but, unfortunately, also to a proportional increase in the heat flux across the channel at the same temperature drop. The change of H with the temperature drop is theoretically described by Eq. (*4*) derived recently[8]

$$\frac{H_2}{H_1} = \left(\frac{\Delta T_1}{\Delta T_2}\right)^{2.8} . \qquad (4)$$

The change of H with the channel thickness w, calculated from Eq. (*1*) by taking into account only the second term on its right-hand side, is

$$\frac{H_2}{H_1} = \left(\frac{w_2}{w_1}\right)^2 . \qquad (5)$$

As a result, an increase in ΔT has a more pronounced effect on the efficiency compared with a decrease in the channel thickness at the expense of the same increase in the heat flux in both cases.

The resolution R_s in FFF is given by[12]

$$R_s = \frac{\sqrt{L}\,|1/R_1 - 1/R_2\,|}{2\left(\sqrt{H_1}/R_1 + \sqrt{H_2}/R_2\right)} , \qquad (6)$$

where $R_{1,2}$ and $H_{1,2}$ are the retention ratio and the plate height, respectively, for species 1 and 2, L is the length of the channel. Equation (*6*) combined with the second term of Eq. (*1*) gives

$$R_s = \left(\frac{\sqrt{L}}{2w\sqrt{\langle v \rangle}}\right)\left[\frac{|1/R_1 - 1/R_2\,|}{\left(\sqrt{\frac{\chi_1}{D_1}}\,/\,R_1 + \sqrt{\frac{\chi_2}{D_2}}\,/\,R_2\right)}\right] . \qquad (7)$$

It follows from Eq. (*7*) that a shortening of the channel accompanied by a corresponding decrease in the average velocity of the carrier liquid keeps the resolution unchanged. As the average velocities in current experiments

are largely above the optimum, due to very low theoretical optimum values, the decrease in the flow rate necessary to compensate the shortening of the channel is not a principal problem. Consequently, the heat flux can be reduced proportionally to the shortening of the channel length. Moreover, further increase in the resolution due to an increase in ΔT can be obtained by a proportional decrease in thickness w and breadth b of the channel by keeping the heat flux unchanged.

The extra-channel contributions to the zone broadening have to be minimized. The zone of the injected sample can be contracted at the entry of the channel by an increase in the temperature drop during the injection. The detection system, including the capillary connecting the channel with the measuring cell, should not increase the total zone width over the uncertainty of the measurement[13]. By assuming that the convenient injection mode can make the contribution due to the injection system negligible, the standard deviation σ_T characterizing the total zone width of a uniform retained species is the sum of the contributions due to the channel, σ_C, and detector, σ_D.

$$\sigma_T^2 = \sigma_C^2 + \sigma_D^2 \tag{8}$$

As the uncertainty of the determination of σ_T lies usually within 1 to 2%, the σ_D can be as high as 20% of σ_C. The theoretical σ_C expressed in volume units can be calculated from[8]

$$\sigma_C^2 = \left(\frac{2D}{R\langle v \rangle} + \frac{\chi w^2 \langle v \rangle}{D} \right) \frac{V_0^2}{R^2 L} . \tag{9}$$

The standard deviation σ_C characterizes the zone width of a uniform species undergoing the dispersive processes exclusively inside the channel and $V_0 \approx wLb$ is the void volume of the channel. The standard deviation at optimum average velocity is[8]

$$\sigma_{C,opt} = \left[Lb^2 w^3 \sqrt{\frac{8\chi}{R^5}} \right]^{0.5} . \tag{10}$$

If the average velocity is higher than the optimum, the first term on the right-hand side of Eq. (*1*), corresponding to the longitudinal diffusion, can be neglected and the result is

$$\sigma_C = \left[Lb^2 w^4 \frac{\chi \langle v \rangle}{DR^2} \right]^{0.5} . \qquad (11)$$

Equation (*11*) shows clearly that miniaturization of the TFFF channel can improve the performance of this technique if the detection system is conveniently designed.

EXPERIMENTAL

The apparatus for the micro-TFFF consisted of an intelligent pump model PU-980 (Jasco, Japan), the injection valve Model 7410 (Rheodyne, U.S.A.) equipped with a 1 μl loop, the UV-VIS variable wavelength intelligent detector model UV-975 (Jasco, Japan) with the measuring cell of 1 μl, and the recorder-integrator Model HP 3395 (Hewlett–Packard, U.S.A.).

The versatile micro-TFFF channel was described in our previous paper[8]. Its dimensions in this study were 100 μm × 5 mm × 100 mm. The cold wall temperature was controlled and kept constant during one separation by using a compact, low-temperature thermostat model RML 6 B (Lauda, Germany). The electric power for heating cartridge was regulated by an electronic variator for both constant and time-programmed temperature drop operations. The temperatures of the cold and hot walls were measured with a digital thermometer (Hanna Instruments, Portugal) equipped with two thermocouples.

The PS standards of various molar masses (Polysciences, Inc., U.S.A., Knauer, Germany, and Waters Associates, U.S.A.) were used as model samples. The tetrahydrofuran (THF) for HPLC (Carlo Erba, Italy) was used as a carrier liquid, the flow rate in micro-TFFF experiments was 10 μl/min.

RESULTS AND DISCUSSION

Micro-TFFF at Constant ΔT and at Programmed Decrease in ΔT

An adequate demonstration of the performance of the micro-TFFF can be provided by separation of PS of a narrow molar mass distribution (MMD). Such experiments were carried out with various mixtures of PS within an extended range of molar masses from 50×10^3 to 10×10^6 g/mol, either under the conditions of constant temperature drop ΔT during the run or with a time-programmed decrease in ΔT. The other experimental conditions, in particular the concentration and volume of the injected polymer solutions, were optimized as in our recent study[8] in order to minimize their effect on the micro-TFFF. The flow rate of the carrier liquid was chosen in agreement with our previous investigation[14] to avoid the casual appearance of the disturbing focusing effect[15] or of the shear degradation[16] of polymer chains. The fractograms in Fig. 1 demonstrating the obtained resolutions can be compared with some chromatograms obtained on a standard (250 mm long

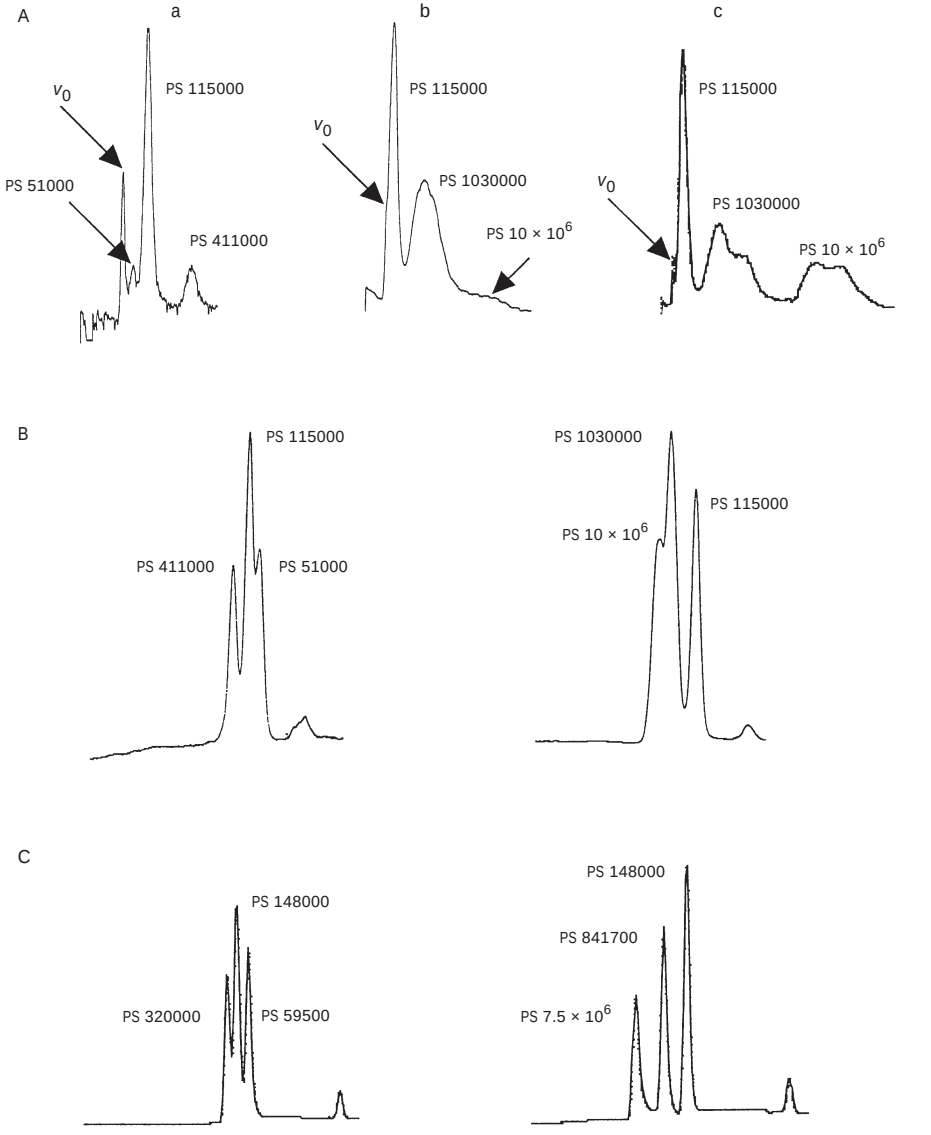

FIG. 1

Comparison of the resolution in separation of three PS by micro-TFFF (A), standard SEC (B) and high-performance SEC (C). Micro-TFFF: Constant ΔT = 35 (a) and 21 K (b); Programmed ΔT = 40 to 10 K (c). Standard SEC: Experimental chromatograms. High-performance SEC: Virtual chromatograms obtained by superposition of the chromatograms provided by the manufacturer[17]

and 8 mm i.d., mixed gel) size exclusion chromatography (SEC) column and with the chromatograms provided by the manufacturer[17] of high-performance SEC columns which were superposed to demonstrate a virtual separation of the PS mixtures of similar molar masses to those in our real micro-TFFF and SEC experiments.

A comparison of the resolution achieved on micro-TFFF channel at constant ΔT = 35 K for medium molar masses ranging from 51×10^3 to 411×10^3 g/mol with that obtained on our standard SEC column demonstrates that the performance of the micro-TFFF is superior to standard SEC. On the other hand, the resolution of virtual separation on high-performance SEC column can be regarded as comparable with the micro-TFFF experiment when taking into account that molar masses of the PS samples separated by SEC are slightly closer to each other in comparison with those separated by micro-TFFF. About the same can be concluded for the comparison of the resolution of the PS 115×10^3 and PS 1.03×10^6 g/mol achieved at constant ΔT = 40 K on micro-TFFF channel (not shown in Fig. 1) with those obtained with SEC. However, the retention of the 10×10^6 g/mol PS in micro-TFFF at this temperature drop was very high. Consequently, the selectivity of the micro-TFFF is clearly superior to any SEC column. The normalized selectivity defined by

$$S_n = \frac{\Delta R}{\Delta \log M}, \qquad (12)$$

where M is the molar mass, can be used to quantitatively compare the micro-TFFF and SEC results. The S_n values, calculated for some typical micro-TFFF experiments, for our standard SEC column, and for the best individual pore size SEC columns[17] as well as for a high-perfomance mixed gel SEC column[17], given in Table I, clearly indicate that only the individual pore size SEC columns exhibit the normalized selectivities close to those currently achieved in micro-TFFF at constant ΔT. While the relatively narrow molar mass range covered by an individual pore size SEC column can be changed only by changing the column, the micro-TFFF is more versatile because a change of the molar mass range can be achieved by changing simply the ΔT. The normalized selectivity values in Table I, calculated for the separation of ultrahigh-molar-mass (UHMM) PS by the micro-TFFF with a programmed decrease in ΔT (shown in Fig. 1), are all higher than the selectivity of any mixed gel high-performance SEC column[17] exhibiting the same resolution achieved at a comparable time of separation. As a result, the newborn micro-TFFF inherits the high performance of the classic[1] TFFF

carried out in standard-size channels but opens much higher variability of the operational conditions that can be chosen to optimize each particular separation, as will be demonstrated in the following paragraph.

Micro-TFFF of UHMM Polymers at Different Temperatures of the Cold Wall

The temperature of the cold wall is an important factor, besides the temperature drop ΔT, influencing the retention due to the fact that the retained species are usually accumulated near the cold wall. Although many experimental studies of TFFF were carried out at various temperatures of the cold wall, the only systematic investigation of the effect of the cold wall temperature on the retention of lipophilic polymers within a limited range of molar masses and cold wall temperatures was performed by Myers *et al.*[18] Later on, Chao *et al.*[19] considered the influence of the cold wall temperature on the so-called "universal calibration". We have examined the effect of the cold wall temperature under the conditions of micro-TFFF by covering the range of the UHMM polymers and by working at as low cold wall temperature as 275 K. The typical results in Fig. 2 show the increase in the average retention ratio R_{ave} (a decrease in the retention) with increasing temperature of the cold wall for both UHMM PS samples. A similar tendency was already observed by Myers *et al.*[18] for the molar masses up to roughly one million. The average retention ratio was calculated from

TABLE I
Normalized selectivities of different separation systems

Separation method	Molar mass range, g/mol	S_n
micro-TFFF, constant ΔT	115000–411000	0.46
micro-TFFF, constant ΔT	115000–1.03×10^6	0.41
micro-TFFF, programmed ΔT	115000–1.03×10^6	0.35
micro-TFFF, programmed ΔT	1.03×10^6–10×10^6	0.12
micro-TFFF, programmed ΔT	115000–10×10^6	0.23
High-performance SEC, mixed gel	1000–10×10^6	0.079
High-performance SEC, individual pore size gel	1000–50000	0.30
	50000–1×10^6	0.30
	1×10^6–10×10^6	0.30

$$R_{ave} = \frac{V_0 \sum h_i}{\sum h_i V_i} , \qquad (13)$$

where the h_i are the heights of the fractogram at the corresponding retention volumes V_i.

According to the theory[1,20,21], a change of the retention in FFF leads to a change of the resolution. This assumption was verified experimentally for very different FFF techniques[2]. However, simultaneous variation of the diffusion coefficient D and of the thermal diffusion coefficient D_T of the retained species, of the viscosity of the carrier liquid, and of the relative viscosity of the polymer solution within the retained zone with temperature influence not only the retention but also the dispersive processes.

Consequently, an evaluation of the effect of the retention changes caused by variation of the cold wall temperature on the resolution is difficult because many empirical or semiempirical rules have to be taken into account. These rules concern the relationship between the molecular characteristics of the polymers and their diffusion coefficients, the temperature dependence of the viscosity of the carrier liquid as well as of the viscosity of polymer solution reflecting the interactions between the macromolecular coils and the solvent. On the other hand, the product of the average retention ratio R_{ave} and of the standard deviation σ, characterizing the width of the

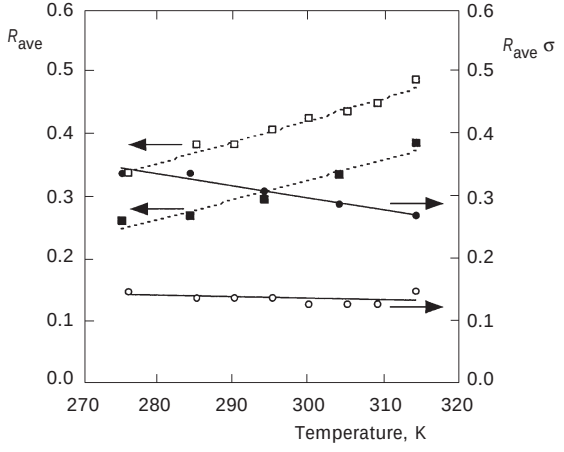

FIG. 2

Effect of the cold wall temperature on the average retention ratio and on the product of the average retention ratio and standard deviation of the zone width for two UHMM PS: ❍, ❑ PS 1.03×10^6; ●, ■ 10×10^6

fractogram of a retained species determined experimentally can clearly indicate the effect of the cold wall temperature on the resolution. The standard deviation σ was calculated from

$$\sigma = \left[\frac{\sum h_i (V_i - V_{ave})^2}{\sum h_i} \right]^{0.5}, \qquad (14)$$

where V_{ave} is the reciprocal value of R_{ave} by imposing a normalization condition $V_0 = 1$.

The experimental investigation of the effect of the cold wall temperature revealed the fact that the R_{ave} and σ change with the increasing cold wall temperature, as can be seen in Fig. 2 for the R_{ave}. However, the product $R_{ave}\,\sigma$ does not exhibit a significant variation with temperature for PS 1.03×10^6 g/mol. Its minor decrease with increasing cold wall temperature for PS 10×10^6 g/mol shows that a higher resolution could be achieved for UHMM samples at a higher cold wall temperature and in a shorter time of the fractionation when the micro-TFFF is carried out at constant ΔT. Figure 3 shows only a small decrease of resolution with increasing cold wall temperature when fractionating a mixture of three PS including one UHMM sample by the micro-TFFF at constant ΔT but the time of the fractionation shortens substantially.

Resolution in SEC, TFFF and Micro-TFFF

A comparison of the SEC chromatograms with the micro-TFFF fractograms of PS mixtures offered a good demonstration of the resolution of these techniques. However, a quantitative evaluation of the resolution can be provided by calculating the polydispersity indexes M_w/M_n of PS samples from the chromatograms or fractograms. The M_w and M_n are the weight-average and number-average molar masses, respectively. A difficulty of such a comparison lies in the uncertainty of the polydispersity indexes M_w/M_n determined by the light scattering and osmometry because the precision of these methods is lower compared with SEC or TFFF [22]. The only convenient solution is to use strictly identical PS samples for the comparison of the resolutions of the examined methods. By coincidence, we had such a possibility to compare our former results from high-performance SEC [23], standard TFFF [24], recent standard SEC and micro-TFFF for few PS samples.

The polydispersity indexes M_w/M_n given in Table II demonstrate that the resolution obtained with micro-TFFF is at least comparable with that of the

standard size TFFF channel (*cf.* the data for PS 111000, PS 411000 and PS 498000 samples) under optimum experimental conditions (namely ΔT). The polydispersity indexes M_w/M_n obtained with our former high-performance SEC column as well as with our recent standard SEC column are systematically higher compared with our new micro-TFFF. Moreover, the M_w values calculated from micro-TFFF or TFFF fractograms seem to be more coherent and systematically closer to the manufacturer's data compared with the data from SEC. The time of separations were 12–20 min for our recent standard SEC, 5–10 h for our former high resolution SEC, 15–30 min

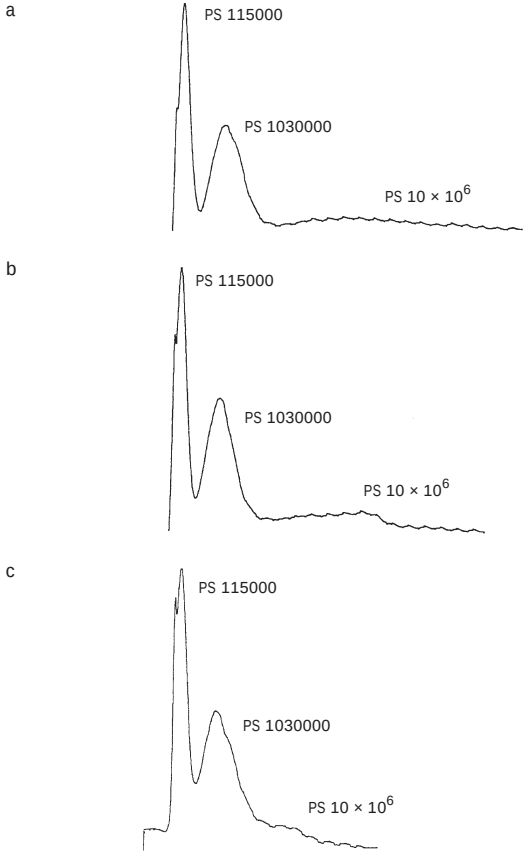

FIG. 3
Comparison of the resolution in separation of three PS by micro-TFFF at different temperatures (T = 300 (a), 305 (b) and 310 K (c)) of the cold wall and at constant ΔT = 20 K

for micro-TFFF, and 3–6 h for our former standard TFFF. The resolutions and separation times clearly demonstrate the high performance of micro-TFFF. Moreover, the PS standards used in this long-term study show a surprising stability during almost three decades thus proving their exceptional quality.

CONCLUSION

Theoretical analysis of the effect of miniaturization of the separation channel revealed the possibility of increasing the performance of TFFF. The increasing the temperature drop across the channel has a more significant impact on the efficiency compared with a decrease in the channel thickness. A substantial decrease in the heat flux across the micro-TFFF channel permits to work at lower temperatures of the cold wall. The low cold wall temperatures do not seem to result in an increase in resolution but higher cold wall temperatures permit to shorten the time of separation. As a result, although the low cold wall temperature that can be reached with micro-TFFF probably does not represent an advantage whenever high-performance and high-speed analysis is the main objective of the fractionation, such a performance can be crucial for fundamental studies of thermal diffusion and this result was obtained only by this technique. The experiments with the micro-TFFF channel confirmed that the resolution is comparable with that obtained with classic size channels but the time of

TABLE II
Comparison of average molar masses obtained from SEC, TFFF and micro-TFFF experiments

Experiment	PS 111000		PS 115000		PS 411000		PS 498000		PS 1030000	
	$M_w \times 10^{-3}$	M_w/M_n	$M_w \times 10^{-3}$	M_w/M_n	$M_w \times 10^{-3}$	M_w/M_n	$M_w \times 10^{-3}$	M_w/M_n	$M_w \times 10^{-3}$	M_w/M_n
SEC[a]	108	1.16	–	–	398	1.11	526	1.15	–	–
SEC	155	1.16	128	1.13	443	1.15	632	1.15	1300	1.28
TFFF[b] ΔT = 40 K	103	1.03	–	–	–	–	–	–	–	–
TFFF[b] ΔT = 40 K	125	1.29	–	–	415	1.11	482	1.17	–	–
micro-TFFF ΔT = 40 K	95	1.12	105	1.13	378	1.09	471	1.08	1155	1.14
micro-TFFF ΔT = 33 K	–	–	130	1.17	408	1.08	–	–	–	–

[a] Earlier experimental results[23]. [b] Earlier experimental results[24].

separation can be reduced. The manipulation in micro-TFFF is simpler, the channel is more versatile, and the sample amount needed for one separation is as small as few nanograms.

REFERENCES

1. Thompson G. H., Myers M. N., Giddings J. C.: *Sep. Sci.* **1967**, *2*, 797.
2. Janča J.: *Field-Flow Fractionation: Analysis of Macromolecules and Particles*. Marcel Dekker, Inc., New York 1988.
3. Schimpf M. E., Caldwell K. D., Giddings J. C.: *Field-Flow Fractionation Handbook*. John Wiley & Sons, New York 2000.
4. Giddings J. C., Martin M., Myers M. N.: *J. Chromatogr.* **1978**, *158*, 419.
5. Giddings J. C.: *J. Microcolumn Sep.* **1993**, *5*, 497.
6. Shiundu P. M., Giddings J. C.: *J. Chromatogr., A* **1995**, *715*, 117.
7. Mes E. P. C., Tijssen R., Kok W. Th.: *J. Chromatogr., A* **2001**, *907*, 201.
8. Janča J.: *J. Liq. Chromatogr. Rel. Tech.* **2002**, *25*, 683.
9. Edwards T. L., Gale B. K., Frazier A. B.: *Anal. Chem.* **2002**, *74*, 1211.
10. Hovingh M. E., Thompson G. H., Giddings J. C.: *Anal. Chem.* **1970**, *42*, 195.
11. Giddings J. C., Yoon Y. H., Caldwell K. D., Myers M. N., Hovingh M. E.: *Sep. Sci.* **1975**, *10*, 447.
12. Martin M., Jaulmes A.: *Sep. Sci. Technol.* **1981**, *16*, 691.
13. Janča J.: *J. Liq. Chromatogr.* **1981**, *4*, 181.
14. Janča J., Martin M.: *Chromatographia* **1992**, *34*, 125.
15. Giddings J. C., Li S., Williams P. S., Schimpf M. E.: *Makromol. Chem., Rapid Commun.* **1988**, *9*, 817.
16. Chubarova E. V., Nesterov V. V. in: *Strategies in Size Exclusion Chromatography* (M. Potschka ans P. L. Dubin, Eds). *ACS Symp. Ser.* **1996**, *635*, 127.
17. Polymer Laboratories, Inc.: www.polymerlabs.com.
18. Myers M. N., Chao W., Chen Ch.-I., Mumar V., Giddings J. C.: *J. Liq. Chromatogr. Rel. Tech.* **1997**, *20*, 2757.
19. Chao W., Williams P. S., Myers M. N., Giddings J. C.: *Anal. Chem.* **1999**, *71*, 1597.
20. Giddings J. C.: *J. Chem. Phys.* **1968**, *49*, 81.
21. Giddings J. C., Yoon Y. H., Caldwell K. D., Myers M. N., Hovingh M. E.: *Sep. Sci.* **1975**, *10*, 447.
22. Janča J.: *Adv. Chromatogr.* **1980**, *19*, 38.
23. Janča J., Kolínský M., Mrkviaková L.: *J. Chromatogr.* **1976**, *121*, 23.
24. Janča J., Klepárník K.: *Sep. Sci. Technol.* **1981**, *16*, 657.